Influence of Liquid Dynamics on the Band Broadening and Time Evolution of Vibrational Excitations for Delocalized Vibrational Modes in Liquids†

Hajime Torii*

Department of Chemistry, School of Education, Shizuoka University, 836 Ohya, Shizuoka 422-8529, Japan

Received: May 4, 2001; In Final Form: July 2, 2001

A theoretical method for treating the effects of liquid dynamics on vibrational band profiles is developed for the situation where resonant intermolecular vibrational interactions are operating. The liquid dynamics is simulated by the molecular dynamics (MD) technique, and the coupled vibrational Hamiltonian is constructed at each time step of the MD runs. Time evolution of delocalized IR and Raman excitations caused by this time-dependent coupled vibrational Hamiltonian is calculated to obtain IR and Raman band profiles as the Fourier transform of the corresponding time correlation functions. This method is applied to the case of the C═O stretching band of neat liquid acetone, a typical case where the effect of resonant intermolecular vibrational interactions is known to be significant. The noncoincidence effect observed in this band is well reproduced. In addition, a better agreement between the observed and calculated bandwidths is obtained by using the present method as compared to the result of the calculation using only static liquid structures. As such, the present method is suggested to be a useful one for treating the effects of liquid dynamics on vibrational band profiles when the vibrations are resonantly coupled. The time scale of the modulation of vibrational eigenstates caused by the liquid dynamics is also discussed.

1. Introduction

Molecular vibrational motions in the liquid phase are more or less mutually coupled because of intermolecular vibrational interactions. In the resonant case, where the intermolecular vibrational interactions are sufficiently large as compared to the difference between the intrinsic vibrational frequencies of the interacting vibrations, the vibrational modes are delocalized. Such delocalization of vibrational modes manifests itself most clearly in the noncoincidence effect (NCE) of vibrational bands. The NCE is the phenomenon that the frequencies of the infrared (IR), isotropic Raman, and anisotropic Raman components of a vibrational band do not coincide. It is observed in many polar bond-stretching bands of neat liquids, such as the C═O stretching band of liquid acetone,[1−4] the amide I bands of liquid formamide[5,6] and *N*,*N*-dimethylacetamide,[7] the C−O and O−H stretching bands of liquid methanol,[8,9] the S═O stretching band of liquid dimethyl sulfoxide,[10] and so forth. It is also observed in vibrational bands of liquid mixtures, such as the C═O stretching band of an acetone-CCl_4 binary mixture,[11,12] and in those of solvent molecules in solution, such as the O−H stretching band of a methanol solution of LiCl or LiBr.[13,14]

The mechanism that gives rise to the NCE may be summarized as follows.[15] When there are *N* molecules (of the same species) in a liquid system, there are *N* vibrational modes arising from the same molecular vibration. These vibrational modes are delocalized and appear at different frequencies if the vibrational motions of neighboring molecules interact resonantly with each other. Since the vibrational patterns (the relative magnitudes and phases of molecular vibrations) of these delocalized modes are different from mode to mode, their IR, isotropic Raman, and anisotropic Raman intensities are also different. As a consequence, vibrational modes with strong isotropic Raman intensities may be located at different frequency positions from those with strong anisotropic Raman intensities or those with strong IR intensities. The NCE occurs in this way.

In many cases, such as the vibrational bands listed above as examples, the most important type of intermolecular vibrational interactions for the occurrence of NCE is the transition dipole coupling (TDC),[15−18] which is a harmonic electrostatic interaction between molecular vibrations. The formula for the potential energy arising from dipole−dipole interactions between molecules *m* and *n* is expressed as

$$V_{mn} = \frac{\boldsymbol{\mu}_m \cdot \boldsymbol{\mu}_n - 3(\boldsymbol{\mu}_m \cdot \mathbf{n}_{mn})(\boldsymbol{\mu}_n \cdot \mathbf{n}_{mn})}{{R_{mn}}^3} \tag{1}$$

where μ_m and μ_n are the dipole moments of molecules *m* and *n*, $\mathbf{n}_{mn}$ is the unit vector along the line connecting the two dipoles, and R_{mn} is the distance between the two dipoles. The formula for the TDC is derived from this equation as the second derivative with respect to the vibrational coordinates of molecules *m* and *n*, which are denoted as Q_m and Q_n. It is given as[19]

$$F_{mn} = \frac{\partial^2 V_{mn}}{\partial Q_m \partial Q_n} = \frac{\left(\frac{\partial \boldsymbol{\mu}_m}{\partial Q_m}\right) \cdot \left(\frac{\partial \boldsymbol{\mu}_n}{\partial Q_n}\right) - 3\left[\left(\frac{\partial \boldsymbol{\mu}_m}{\partial Q_m}\right)\cdot \mathbf{n}_{mn}\right]\left[\left(\frac{\partial \boldsymbol{\mu}_n}{\partial Q_n}\right)\cdot \mathbf{n}_{mn}\right]}{{R_{mn}}^3} \tag{2}$$

This mechanism is called TDC, because the dipole derivatives appearing in this formula are related within the harmonic approximation to the transition dipole for the vibrational

† Part of the special issue "Mitsuo Tasumi Festschrift".

* To whom correspondence should be addressed. Telephone: +81-54-238-4624. Facsimile: +81-54-237-3354. E-mail: torii@ed.shizuoka.ac.jp.

10.1021/jp011688k CCC: $22.00
Published on Web 08/29/2001

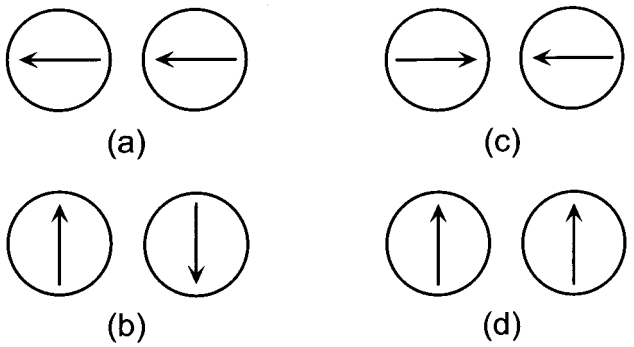

Figure 1. Scheme of typical cases where negative [(a) and (b)] and positive [(c) and (d)] resonant intermolecular vibrational interactions are operating according to the TDC mechanism. The transition dipoles of molecules are denoted by arrows.

transition between $v = 0$ and 1 as

$$\langle 0|\boldsymbol{\mu}|1\rangle = \left(\frac{\partial \boldsymbol{\mu}}{\partial Q}\right)\langle 0|\ Q\ |1\rangle \tag{3}$$

According to eq 2, the signs and magnitudes of intermolecular vibrational interactions strongly depend on the relative positions and orientations of the interacting molecules, as shown schematically in Figure 1. As a result, the phenomena arising from the TDC mechanism are sensitive to liquid structures.[15] In previous studies, the NCE has been analyzed theoretically for neat liquids, binary liquid mixtures, and solutions by calculating the IR and polarized Raman spectra on the basis of the TDC mechanism and the liquid structures derived from Monte Carlo (MC) or molecular dynamics (MD) simulations.[15,20−24] By using this method, called the MC/TDC or MD/TDC method, the relation between the signs and magnitudes of the NCE and the liquid structures has been clarified.

In the above studies, it has been shown that resonant intermolecular vibrational interactions also induce broadening of vibrational bands.[15,24] The IR and anisotropic Raman bands are broadened to a greater extent than the isotropic Raman band. As a result, additional broadening of IR and anisotropic Raman bands as compared to the isotropic Raman band cannot be simply related to rotational relaxation for resonantly interacting vibrations, although the simple relation holds for vibrations of solutes in dilute solutions. As shown in ref 24, the band broadening arising from resonant intermolecular vibrational interactions is related to the time evolution of transient absorption anisotropy observed in an IR pump−probe experiment.[25] The relation that holds for dilute solutions between the behavior of optical signals and rotational relaxation cannot be used for resonantly interacting vibrations also in the time domain as well as in the frequency domain.

It is expected, however, that vibrational bandwidths are affected by rotational relaxation to a certain extent even when the vibrations are resonantly coupled. A problem arises as to how such effects are treated, because intermolecular vibrational interactions are also affected by molecular rotations. For example, suppose that two molecules are located as shown in Figure 1a. When the molecule on the left-hand side rotates by 180°, we get the situation shown in Figure 1c, with a positive instead of negative intermolecular vibrational interaction. It is therefore understandable that molecular rotations in liquids accompany changes in the intermolecular vibrational interactions and, hence, in the vibrational patterns of delocalized vibrational modes. If the changes in the vibrational patterns are significant, effects of rotational relaxation on vibrational spectra cannot be simply treated by orientational correlation functions of individual molecules.

In the present study, a new theoretical method for treating the effects of liquid dynamics (molecular translations and rotations) on vibrational band profiles is developed for the situation where resonant intermolecular vibrational interactions are operating. In contrast to the theoretical methods employed in the previous studies on this subject,[26−28] it is possible to treat all the three components (IR, isotropic Raman, and anisotropic Raman) of a vibrational band simultaneously, and to calculate both the frequency positions (including the magnitude of the NCE) and the bandwidths. As an example of the application of the present method, we show the case of the C═O stretching band of neat liquid acetone, a typical case where the NCE is clearly observed. It is demonstrated that a better agreement is obtained between the observed and calculated bandwidths by using this method as compared to the calculations using only static liquid structures.

2. Theory

In the present study we examine the effects of liquid dynamics (intermolecular vibrational motions consisting of molecular translations and rotations) on the band profiles of high-frequency delocalized vibrational excitations (intramolecular vibrations coupled intermolecularly), but assume that the latter vibrational excitations do not have any effects on the former. This assumption is considered to be valid for thermally inaccessible vibrational excitations, such as the C═O stretching mode of acetone treated in the example shown below. In this case, since the positions of the molecules and the orientations of their transition dipoles are time dependent, the intermolecular vibrational interactions are also time dependent, as explained in the previous section. In other words, we have to treat the Hamiltonian for the vibrational excitations as time dependent according to liquid dynamics. The delocalized normal modes obtained by diagonalization of the Hamiltonian at time $t = 0$ are different from those at later time.

The IR spectrum is expressed as[29]

$$I^{(\mathrm{IR})}(\omega) = Re \int_0^\infty \mathrm{d}t\, \exp(i\omega t)\langle \boldsymbol{\mu}(t)\boldsymbol{\mu}(0)\rangle \tag{4}$$

where $\boldsymbol{\mu}(t)$ is the dipole operator at time t, and the bracket denotes statistical average. In the case of the vibrational bands of solutes in dilute solutions, it is sufficient to calculate $\langle \boldsymbol{\mu}(t)\boldsymbol{\mu}(0)\rangle$ for individual molecules, because the molecular motions of the solutes in such solutions may be considered to be independent of each other. However, such a simple treatment is not considered to be valid when the vibrational motions are resonantly coupled.

The time evolution of $\boldsymbol{\mu}(t)$ is expressed as[29]

$$\boldsymbol{\mu}(t) = U^\dagger(t)\boldsymbol{\mu}U(t) \tag{5}$$

where $\boldsymbol{\mu} \equiv \boldsymbol{\mu}(0)$, and

$$U(t) = \exp_+\left[-\frac{i}{\hbar}\int_0^t \mathrm{d}\tau\, H(\tau)\right] \tag{6}$$

$$U^\dagger(t) = \exp_-\left[\frac{i}{\hbar}\int_0^t \mathrm{d}\tau\, H(\tau)\right] \tag{7}$$

where $H(\tau)$ is the time-dependent Hamiltonian for the vibrational excitations. For the modes with $\hbar\omega \gg kT$, we only have to evaluate

$$\langle 0|\boldsymbol{\mu} U(t)\boldsymbol{\mu}|0\rangle = \sum_{p=1}^{3}\langle 0|\mu_p U(t)\mu_p|0\rangle \quad (8)$$

and take the statistical average to calculate the IR spectrum, where $|0\rangle$ is the wave function of the ground state.

The quantum mechanical bracket appearing on the right-hand side of eq 8 may be evaluated as

$$\langle 0|\mu_p U(t)\mu_p|0\rangle = \sum_{\xi,\zeta=1}^{N}\langle 0|\mu_p|\zeta_t\rangle\langle\zeta_t|U(t)|\xi_0\rangle\langle\xi_0|\mu_p|0\rangle \quad (9)$$

where $|\zeta_t\rangle$ and $|\xi_t\rangle$ are eigenstates of the system at time t. The wave function defined as

$$|\psi_p^{(\mathrm{IR})}(0)\rangle = \sum_{\xi=1}^{N}|\xi_0\rangle\langle\xi_0|\mu_p|0\rangle \quad (10)$$

is the one formed at time $t = 0$ by the interaction with the radiation polarized in the pth direction. The vibration represented by this wave function is one of the IR intensity-carrying modes,[30] and plays the role of the doorway state in the IR excitation process.[31] The operator $U(t)$ represents the time evolution of this wave function as

$$|\psi_p^{(\mathrm{IR})}(t)\rangle = U(t)|\psi_p^{(\mathrm{IR})}(0)\rangle \quad (11)$$

In numerical calculations, $U(t)$ is expressed as a product of short-time evolutions by assuming that the Hamiltonian is essentially invariant during a very short time period. We obtain

$$|\psi_p^{(\mathrm{IR})}(\tau+\Delta\tau)\rangle = \exp\left[-\frac{i}{\hbar}\Delta\tau\, H(\tau)\right]|\psi_p^{(\mathrm{IR})}(\tau)\rangle$$

$$= \sum_{\xi=1}^{N}|\xi_\tau'\rangle\exp[-i\omega_\xi(\tau)\Delta\tau]\langle\xi_\tau|\psi_p^{(\mathrm{IR})}(\tau)\rangle \quad (12)$$

where $\omega_\xi(\tau)$ is the vibrational frequency for the eigenstate $|\xi_\tau\rangle$, and $|\xi_\tau'\rangle$ is the wave function with the same amplitudes of molecular vibrations as $|\xi_\tau\rangle$ but with the molecular orientations evaluated at time $\tau + \Delta\tau$. We take $\Delta\tau$ as the time step of the MD simulation in the calculation shown below. We construct $H(\tau)$ every time step, diagonalize this Hamiltonian to get $\omega_\xi(\tau)$ and $|\xi_\tau\rangle$, and calculate the time evolution of vibrational excitations according to eq 12.

The Raman spectrum is calculated in a similar way. The spectrum arising from the pq element of the polarizability operator α_{pq} is expressed as

$$I_{pq}^{(\mathrm{R})}(\omega) = Re\int_0^\infty \mathrm{d}t\,\exp(i\omega t)\left\langle\langle 0|\alpha_{pq}U(t)\alpha_{pq}|0\rangle\right\rangle \quad (13)$$

The quantum mechanical bracket on the right-hand side of this equation is calculated as

$$\langle 0|\alpha_{pq}U(t)\alpha_{pq}|0\rangle = \sum_{\xi,\zeta=1}^{N}\langle 0|\alpha_{pq}|\zeta_t\rangle\langle\zeta_t|U(t)|\xi_0\rangle\langle\xi_0|\alpha_{pq}|0\rangle \quad (14)$$

In the same way as in eqs 10 and 11, this equation may be interpreted as representing the time evolution of a Raman excitation

$$|\psi_{pq}^{(\mathrm{R})}(t)\rangle = U(t)\,|\psi_{pq}^{(\mathrm{R})}(0)\rangle \quad (15)$$

where $|\psi_{pq}^{(\mathrm{R})}(0)\rangle$, the wave function formed by the Raman excitation at time $t = 0$, is defined as

$$|\psi_{pq}^{(\mathrm{R})}(0)\rangle = \sum_{\xi=1}^{N}|\xi_0\rangle\langle\xi_0|\alpha_{pq}|0\rangle \quad (16)$$

Numerical evaluation of this time evolution is carried out in the same way as shown in eq 12 for IR excitations.

3. Computational Procedure

Calculations of the IR and Raman spectra in the C═O stretching region of neat liquid acetone were carried out in the following three steps: (1) MD simulations of liquid structures and dynamics, (2) calculations of time correlation functions (the integrands of eqs 4 and 13), and (3) Fourier transformation of the time correlation functions. This method will be called the MD/TDC/WFP method, where WFP stands for "wave function propagation".

The MD simulations were performed by using the OPLS intermolecular potential function derived by Jorgensen,[32] in which electrostatic interactions between fixed atomic charges and Lennard-Jones interactions are involved. The methyl groups were treated as united atoms. Only intermolecular degrees of freedom were considered. Four-dimensional vectors (quaternions) were used to represent molecular orientations in solving the equations of motion,[33,34] in combination with the leapfrog integration method.[34] The liquid system consisted of 128 molecules in a cubic cell. The periodic boundary condition was employed. The volume of the cubic cell was fixed so that the molecular volume is equal to 126.5 Å^3. The temperature was kept at 293 K by adjusting the total kinetic energy every 200 fs. The time step was set to 2 fs. The system was equilibrated for 40 ps, after which production runs were carried out.

The calculations of the time correlation functions of the dipole and polarizability operators were carried out as described in section 2. To evaluate the time evolutions of the IR and Raman excitations, the **F** matrix (the matrix of vibrational force constants) was constructed every time step by treating each molecule as an oscillator having a transition dipole. All the diagonal elements of the **F** matrix were assumed to be 1.737 mdyn Å^{-1} amu^{-1}, which corresponds to an unperturbed vibrational frequency of 1717 cm^{-1}.[22] The off-diagonal elements were evaluated in terms of the TDC mechanism (eq 2). The eigenstates in the C═O stretching band for the liquid structure at each time step were calculated by diagonalization of the **F** matrix (with size 128 × 128) thus constructed. The dipole derivative of the C═O stretching mode (related to the vibrational transition dipole as given in eq 3), which is parallel to the C═O bond, was placed at the center of the C═O bond of each molecule. The magnitude of the dipole derivative was assumed to be 2.08 D Å^{-1} amu$^{-1/2}$,[15,22] which is consistent with the observed IR intensity.[35] The Raman tensor (the polarizability tensor bracketed by the wave functions of the ground and excited vibrational states) of the C═O stretching mode of each molecule was assumed to be axially symmetric with respect to the C═O bond.

In contrast to the previous studies,[15,20−24] where IR and Raman spectra were calculated as the statistical average of those for a few hundred samples of instantaneous liquid structures taken from MC or MD simulations and hence only the static aspects of liquid structures were taken into account, vibrational eigenstates were calculated for all the time steps needed to calculate the Fourier transforms of the time correlation functions. To obtain a frequency resolution of about 0.5 cm^{-1}, the time

correlation functions were calculated for about 65.5 ps (32768 time steps). Therefore, **F** matrices were constructed and diagonalized 32768 times to get one sample set of time correlation functions. The statistical average over 50 samples were taken for the time correlation functions. The "time $t = 0$" of each sample was separated from that of another by more than 30 ps to get good statistical average.

The time correlation functions thus calculated were multiplied by a function representing vibrational pure dephasing, expressed as[36]

$$f(t) = \exp\left[-\frac{\Delta^2}{\Lambda^2}\{\exp(-\Lambda t) + \Lambda t - 1\}\right] \qquad (17)$$

where Δ and Λ are the magnitude and the rate of vibrational frequency modulation. We assumed $\Delta = \Lambda = 10.35$ cm^{-1} (i.e., $\kappa \equiv \Lambda/\Delta = 1.0$) in the present study, so that the vibrational line shape function obtained as the Fourier transform of $f(t)$ has a full width at half-maximum (fwhm) of 7.8 cm^{-1}, the width of the C═O stretching isotropic Raman band of acetone diluted in CCl_4 (with the volume fraction of 0.004).[12,37] The assumed value of κ (1.0) is considered to be reasonable, taking into account that the observed isotropic Raman band[12] seems to be in a shape somewhere between Gaussian and Lorentzian.

The time correlation functions of the dipole and polarizability operators multiplied by $f(t)$ were Fourier transformed to obtain the IR and Raman spectra.

As a reference to the above calculations, the IR and Raman spectra in the localized limit and in the static case were also calculated. The spectra in the localized limit were obtained by switching off all the off-diagonal elements of the **F** matrices. In this case, vibrational excitations are localized on individual molecules. The spectra in the static case were obtained by freezing all the liquid dynamics in the calculations of the IR and Raman spectra, i.e., by employing the MD/TDC method developed in the previous studies.[15,20−24]

The calculations were carried out on an NEC SX-3 supercomputer at the Research Center for Computational Science of the Okazaki National Research Institutes.

4. Results and Discussion

The IR and polarized Raman spectra of neat liquid acetone in the C═O stretching region obtained by using the MD/TDC/WFP method developed in the present study are shown in Figure 2a and b. Those calculated for the static case (MD/TDC method) are shown in Figure 2c and d. The NCE is clearly seen in both cases. The magnitude of the NCE (based on the first moments of the isotropic and anisotropic Raman bands) is calculated to be 5.6 cm^{-1} in the former (dynamic) case and 5.7 cm^{-1} in the latter, in good agreement with the observed value (5.2 cm^{-1}).[12] This result indicates that the magnitude of the NCE remains almost the same when the liquid dynamics is taken into account in the calculations. By contrast, the bandwidths are evidently different between the two cases. The calculated bandwidths (fwhm) are summarized on the first and second rows of Table 1. It is noticed that the width of the isotropic Raman band is slightly narrower in the dynamic case than in the static case. This is probably due to a kind of motional narrowing effect as discussed previously.[26,28] The broadening of the IR and anisotropic Raman bands obtained in the dynamic case as compared to the static case is considered to originate mainly from rotational relaxation. Clearly, the anisotropic Raman band is more strongly affected by rotational relaxation than the IR band. The observed bandwidths taken from the literature[4,12,37] are listed on the fourth row. It is clearly recognized from the comparison of the observed and calculated bandwidths that a better agreement is obtained when the liquid dynamics is taken into account in the calculations. A little too large width of the anisotropic Raman band calculated in the dynamic case suggests that the liquid dynamics in the MD simulation is slightly too fast. A better result may be obtained by improving the potential energy function used in the MD simulation.

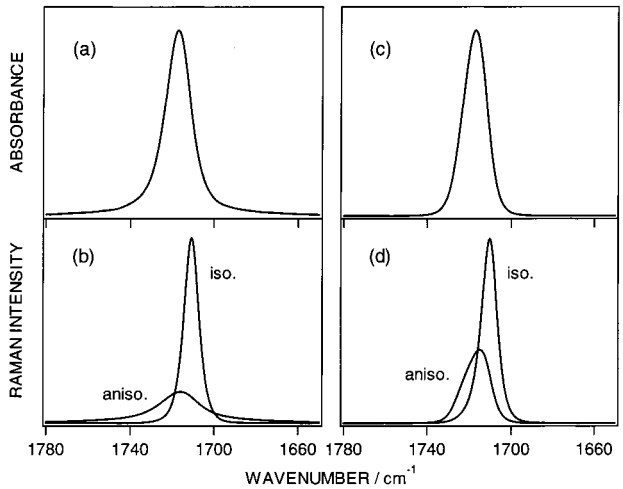

Figure 2. (a) IR and (b) polarized Raman spectra in the C═O stretching region of neat liquid acetone in the delocalized dynamic case calculated by the MD/TDC/WFP method developed in the present study, and (c) IR and (d) polarized Raman spectra in the delocalized static case calculated by the MD/TDC method developed previously.

The larger effect of rotational relaxation on the anisotropic Raman band as compared with the IR band is expected to be seen also in the corresponding time correlation functions of the molecular axes of individual molecules. The time correlation functions of the form

$$C_1(t) = \frac{1}{N}\sum_{m=1}^{N}\langle \mathbf{u}_m(t)\cdot\mathbf{u}_m(0)\rangle \qquad (18)$$

$$C_2(t) = \frac{1}{N}\sum_{m=1}^{N}\left\langle \frac{3}{2}[\mathbf{u}_m(t)\cdot\mathbf{u}_m(0)]^2 - \frac{1}{2}\right\rangle \qquad (19)$$

where $\mathbf{u}_m(t)$ denotes the unit vector along the principal axis (parallel to the C═O bond) of the mth molecule at time t, are relevant to the IR and anisotropic Raman bands, respectively. These time correlation functions calculated for neat liquid acetone are shown in Figure 3. Both correlation functions decay almost exponentially, with slight convex curvatures in the semilog plot around $t = 0$. The time constant of the decay of $C_2(t)$, ∼0.5 ps, is indeed significantly shorter than that of $C_1(t)$, ∼1.7 ps.

Since the faster decay of $C_2(t)$ as compared with $C_1(t)$ can also be obtained from a rotational diffusion model,[38] it may be meaningful to compare the above time constants of $C_1(t)$ and $C_2(t)$ with the time scale of molecular rotation obtained from simple models. In the short-time inertial regime, the time scale of molecular rotation is estimated as $\tau_R \sim (I/3kT)^{1/2}$, where I is the moment of inertia.[39] In the case of an acetone molecule, this time scale is $\tau_R \sim 0.3$ ps, which is shorter than the time constants of $C_1(t)$ and $C_2(t)$. Since the slight convex curvatures of $\ln[C_1(t)]$ and $\ln[C_2(t)]$ are seen only in a very short time interval around $t = 0$, the rotational motions of acetone molecules are not considered to be in the inertial regime in the

TABLE 1: Calculated and Observed Widths of the C═O Stretching Band of Neat Liquid Acetone

	method of calculation		width (fwhm, cm^{-1})		
	liquid structure	C═O stretch mode	IR	isotropic	anisotropic
calculated[a]	dynamic (WFP)	delocalized (TDC)	14.6	8.4	23.9
	static	delocalized (TDC)	13.4	8.8	15.0
	dynamic (WFP)	localized	11.9	(7.8)	19.7
observed			~14[b]	8.5[c]	20.3[c]

[a] After convolution by the line shape function (eq 17) of fwhm = 7.8 cm^{-1} and $\kappa = 1.0$. [b] Reference 4. The spectrum of α_m''. [c] References 12 and 37.

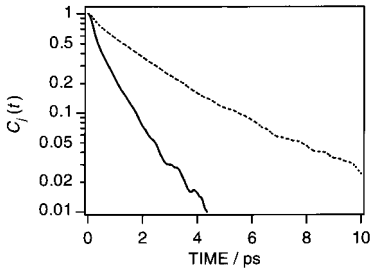

Figure 3. Calculated time correlation functions of the molecular axes of individual molecules (defined by eqs 18 and 19) in neat liquid acetone. Broken line: $C_1(t)$. Solid line: $C_2(t)$.

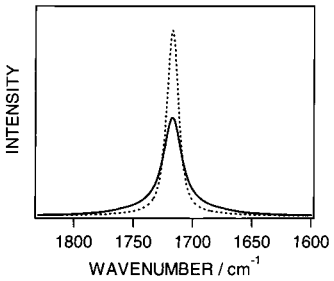

Figure 4. Normalized IR and anisotropic Raman spectra in the C═O stretching region of neat liquid acetone calculated in the localized limit. Broken line: IR. Solid line: anisotropic Raman.

sub-ps time scale. In a simple rotational diffusion model, the time scale of molecular rotational diffusion is estimated as $\tau_D \sim \eta V/kT$, where η is the viscosity and V is the molecular volume.[40] In the case of liquid acetone, this time scale is calculated to be $\tau_D \sim 9$ ps, which is longer than the time constants of $C_1(t)$ and $C_2(t)$. It may be said, therefore, that the functional form and the time scale of the variation of $C_1(t)$ and $C_2(t)$ cannot be explained by such simple models.

The IR and anisotropic Raman bands calculated in the localized limit, where all the off-diagonal vibrational couplings are switched off, are shown in Figure 4. These bands may also be obtained as the Fourier transform of $C_1(t)$ and $C_2(t)$, respectively, multiplied by $f(t)$, the function representing the effect of vibrational pure dephasing (eq 17). The isotropic Raman band in this limit is just the Fourier transform of $f(t)$, since it is not affected by rotational relaxation. The widths of these calculated bands are listed on the third row of Table 1. Comparison of these values with those on the first row demonstrates that all the three components (IR, isotropic Raman, and anisotropic Raman) of the C═O stretching band of neat liquid acetone are more or less broadened by the effect of resonant intermolecular vibrational interactions. The additional band broadening due to this effect amounts to 3−4 cm^{-1} for the IR and anisotropic Raman bands.

A question arises at this point as to whether one can distinguish band-broadening mechanisms only by examining the IR and anisotropic Raman band shapes. Suppose we observe an IR band with the fwhm of 14 cm^{-1} and an anisotropic Raman band with the fwhm of 20 cm^{-1}. In fact, these vibrational bandwidths alone do not specify which band-broadening mechanisms are really operating. One may consider that these bandwidths arise only from vibrational pure dephasing and rotational relaxation as in the localized limit, with slightly faster liquid dynamics than in the present calculation, or one may expect that the effect of resonant intermolecular vibrational interactions is also significant. However, the situation is different when the isotropic Raman band profile is also taken into account. In the localized limit, the isotropic Raman band appears at the same vibrational frequency as the IR and anisotropic Raman bands. In other words, the NCE is not observed in this limit. The sign and the magnitude of the NCE provide information on the resonant intermolecular vibrational interactions. It has been shown in the previous study that the magnitude of band broadening arising from resonant intermolecular vibrational interactions is on the same order of magnitude as the NCE.[24] From a detailed analysis of vibrational bands as described in the present study, it is possible to determine the magnitudes of the effects of different band-broadening mechanisms.

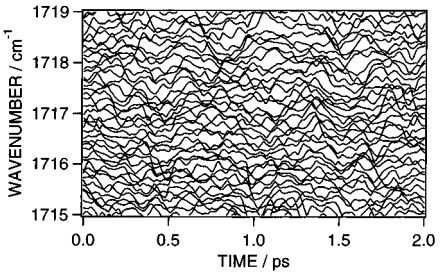

Figure 5. Time evolution of the instantaneous vibrational frequencies of delocalized eigenstates in the C═O stretching band of neat liquid acetone. Only the 1719−1715 cm^{-1} region is shown. A time interval of 2 ps is sampled.

As shown above, the effect of rotational relaxation on the vibrational bandwidths can be seen in the localized limit as well as in the delocalized case. However, the Fourier transform relationship between the vibrational band shapes and the time correlation functions $C_j(t)$ (eqs 18 and 19) that holds in the localized limit is not valid in the delocalized case, because the delocalized vibrational modes are modulated by molecular rotations as explained in section 1. This point is clearly recognized by inspecting the time evolution of the instantaneous vibrational frequencies of eigenstates, which is shown in Figure 5. It is seen that the instantaneous vibrational frequencies of eigenstates are modulated on the time scale of 100 fs or less, with many real and avoided crossings with each other. Such a fast time evolution of instantaneous vibrational frequencies has been shown to occur in the low-frequency part (intermolecular vibrations) for a few liquid systems.[41,42] The present calculation shows that a similar phenomenon is seen also in the high-frequency part (intramolecular vibrations coupled intermolecularly).

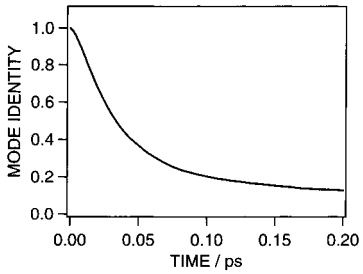

Figure 6. Time correlation function of mode identity (defined in eq 20) calculated for the C═O stretching band of neat liquid acetone.

However, the existence of many crossings of eigenstates alone does not directly indicate that the eigenstates lose their identities rapidly, because, generally speaking, an eigenstate may possibly retain its vibrational pattern after it crosses with another eigenstate. The time scale of the changes in the vibrational patterns of eigenstates is obtained by calculating the time correlation function of "mode identity", expressed as

$$M(t) = \frac{1}{N}\sum_{\xi=1}^{N}\langle \max_{1\le\zeta\le N}\{|\langle\zeta_t|\xi_0\rangle|^2\}\rangle \qquad (20)$$

The result of the calculation of this time correlation function is shown in Figure 6. Obviously, $M(t)$ is identical to unity at $t = 0$, and decreases as the eigenstates lose their identities in later time. In Figure 6 $M(t)$ looks like approaching a finite asymptotic value ($\sim$0.06668) as $t \rightarrow \infty$. In fact, since we have

$$\sum_{\zeta=1}^{N}|\langle\zeta_t|\xi_0\rangle|^2 = 1 \qquad (21)$$

for all $|\xi_0\rangle$ and t, $M(t)$ is always larger than $1/N$. However, we do not have a formula for the asymptotic value of $M(t)$ at present.

It is seen in Figure 6 that the loss of mode identity occurs on the time scale of about 40 fs. This time scale is significantly shorter than that of the rotational relaxation of individual molecules (0.5 or 1.7 ps) shown in Figure 3. This difference in the time scales is noteworthy, considering that the two phenomena arise from the same liquid dynamics. It may be said that vibrational patterns of delocalized modes are more sensitive to liquid dynamics than orientations of individual molecules. This is probably due to the collective nature of the delocalized vibrational modes; since the vibrational motions of many molecules are involved in each delocalized mode, its vibrational pattern will change as the orientations of only a few of these molecules are altered by liquid dynamics. Therefore, the effects of liquid dynamics on the vibrational band profiles of delocalized modes cannot be simply related to the time correlation functions of the orientations of individual molecules.

5. Concluding Remarks

In the present study we have developed a theoretical method, called the MD/TDC/WFP method, for treating the effects of liquid dynamics on vibrational band profiles when resonant intermolecular vibrational interactions are operating. It has been applied to the case of the C═O stretching band of neat liquid acetone. A good agreement has been obtained between the observed and calculated vibrational band profiles (the magnitude of the NCE and the IR and Raman bandwidths).

The MD/TDC/WFP method is the method of choice when delocalized vibrational eigenstates are modulated on a shorter time scale than orientations of individual molecules. As shown in Figures 5 and 6, this is indeed the case for the C═O stretching band of neat liquid acetone. It is expected that the present method will be useful to analyze band-broadening mechanisms in many cases. It is also expected that it will be applicable to simulations of time-domain optical signals of resonantly interacting vibrations. Discussion on this point will be made in future studies.

References and Notes

(1) Fini, G.; Mirone, P. *J. Chem. Soc., Faraday Trans. 2* **1974**, *70*, 1776.
(2) Schindler, W.; Sharko, P. T.; Jonas, J. *J. Chem. Phys.* **1982**, *76*, 3493.
(3) Dybal, J.; Schneider, B. *Spectrochim. Acta A* **1985**, *41*, 691.
(4) Bertie, J. E.; Michaelian, K. H. *J. Chem. Phys.* **1998**, *109*, 6764.
(5) Mortensen, A.; Faurskov Nielsen, O.; Yarwood, J.; Shelley, V. *J. Phys. Chem.* **1994**, *98*, 5221.
(6) Mortensen, A.; Faurskov Nielsen, O.; Yarwood, J.; Shelley, V. *J. Phys. Chem.* **1995**, *99*, 4435.
(7) Thomas, H. D.; Jonas, J. *J. Chem. Phys.* **1989**, *90*, 4144.
(8) Zerda, T. W.; Thomas, H. D.; Bradley, M.; Jonas, J. *J. Chem. Phys.* **1987**, *86*, 3219.
(9) Perchard, C.; Perchard, J. P. *J. Raman Spectrosc.* **1975**, *3*, 277.
(10) Fini, G.; Mirone, P. *Spectrochim. Acta A* **1976**, *32*, 625.
(11) Giorgini, M. G.; Fini, G.; Mirone, P. *J. Chem. Phys.* **1983**, *79*, 639.
(12) Musso, M.; Giorgini, M. G.; Döge, G.; Asenbaum, A. *Mol. Phys.* **1997**, *92*, 97.
(13) Sokolowska, A.; Kecki, Z. *J. Raman Spectrosc.* **1993**, *24*, 331.
(14) Perchard, J. P. *Chem. Phys. Lett.* **1976**, *44*, 169.
(15) Torii, H.; Tasumi, M. *J. Chem. Phys.* **1993**, *99*, 8459.
(16) Torii, H. *J. Mol. Struct. (THEOCHEM)* **1994**, *311*, 199.
(17) McHale, J. L. *J. Chem. Phys.* **1981**, *75*, 30.
(18) Logan, D. E. *Chem. Phys.* **1986**, *103*, 215.
(19) For high-frequency intramolecular modes, such as the C═O stretching mode of acetone, we can safely neglect the contribution of the cross terms ($\partial\boldsymbol{\mu}_m/\partial Q_n$ and $\partial\boldsymbol{\mu}_n/\partial Q_m$) and the derivatives of R_{mn} and $\mathbf{n}_{mn}$ with respect to Q_m or Q_n.
(20) Torii, H.; Tasumi, M. *Bull. Chem. Soc. Jpn.* **1995**, *68*, 128.
(21) Torii, H.; Tasumi, M. *J. Phys. Chem. B* **1998**, *102*, 315.
(22) Torii, H.; Musso, M.; Giorgini, M. G.; Döge, G. *Mol. Phys.* **1998**, *94*, 821.
(23) Torii, H. *J. Phys. Chem. A* **1999**, *103*, 2843.
(24) Torii, H. *Chem. Phys. Lett.* **2000**, *323*, 382.
(25) Woutersen, S.; Bakker, H. J. *Nature* **1999**, *402*, 507.
(26) Döge, G. *Z. Naturforsch.* **1973**, *28a*, 919.
(27) van Woerkom, P. C. M.; de Bleyser, J.; de Zwart, M.; Leyte, J. C. *Chem. Phys.* **1974**, *4*, 236.
(28) Wang, C. H. *Mol. Phys.* **1977**, *33*, 207.
(29) Mukamel, S. *Principles of Nonlinear Optical Spectroscopy*; Oxford University Press: New York, 1995.
(30) Torii, H.; Ueno, Y.; Sakamoto, A.; Tasumi, M. *J. Phys. Chem. A* **1999**, *103*, 5557.
(31) Torii, H.; Tasumi, M. *J. Chem. Phys.* **1992**, *97*, 86.
(32) Jorgensen, W. L.; Briggs, J. M.; Contreras, M. L. *J. Phys. Chem.* **1990**, *94*, 1683.
(33) Evans, D. J. *Mol. Phys.* **1977**, *34*, 317.
(34) Allen, M. P.; Tildesley, D. J. *Computer Simulation of Liquids*; Oxford University Press: Oxford, 1989.
(35) Sun, T. F.; Chan, J. B.; Wallen, S. L.; Jonas, J. *J. Chem. Phys.* **1991**, *94*, 7486.
(36) Kubo, R. *Adv. Chem. Phys.* **1969**, *15*, 101.
(37) Musso, M.; Torii, H.; Giorgini, M. G.; Döge, G. *J. Chem. Phys.* **1999**, *110*, 10076.
(38) Gordon, R. G. *J. Chem. Phys.* **1965**, *43*, 1307.
(39) Lynden-Bell, R. M. *Mol. Phys.* **1978**, *36*, 1529.
(40) Debye, P. *Polar Molecules*; Dover: New York, 1928.
(41) Moore, P.; Space, B. *J. Chem. Phys.* **1997**, *107*, 5635.
(42) David, E. F.; Stratt, R. M. *J. Chem. Phys.* **1998**, *109*, 1375.